DØnote xxxx
Version 1.0
June 5, 2002

Status of PMCS_Muon

Shawn Kwang, Sarah Eno
University of Maryland

Abstract

In this Note, we present the current status of the PMCS_MUON package. The PMCS_MUON package is used to quickly simulate the behaviors of muons in the DØ detector. We also describe how muons in different regions are modeled in each subregion, and we tuned PMCS_MUON from the results of DØ*reco*. Finally, we compare PMCS_MUON's results to the results of DØ*reco*.

Contents

1 Introduction **2**

2 Parameterization Methodology **2**
2.1 Matching Criteria 2
2.2 Detector Regions 2

3 Comparison **3**
3.1 Matching Results 3
3.2 Tuning to DØ*reco* 3
3.3 Efficiency Plots 3

4 Resolutions **4**

5 Conclusion **4**

6 Acknowledgements **4**

List of Tables

1 Detector Regions and Subregions. 5
2 Efficiencies for Flat Subregions. 5
3 Fits of Other Subregions. 6

List of Figures

1 $\Delta\phi$ comparison between PMCS to MC muons and DØ*reco* to MC muons. . . 6
2 $\Delta\eta$ comparison between PMCS to MC muons and DØ*reco* to MC muons. . . 7
3 ΔR calculated from $\Delta\phi$ and $\Delta\eta$. 8
4 Efficiency of Subregion Bottom Foot 2. 9
5 Efficiency of Subregion edge of segment, left side. 10
6 Efficiency of Subregion edge of segment, right side. 11
7 Efficiency of Subregion edge of hole, x dimension. 12
8 Efficiency of Subregion edge of hole, y dimension. 13
9 Comparison between PMCS and DØ*reco* muons in the Central Region, Subregion general central. 14
10 Comparison of Efficiencies for Central Region, all other Subregions. 15
11 Forward Region Efficiency plot for all eight segments. 16
12 Comparison Efficiencies forthe Far Forward Region for x dimension. 17
13 Comparison Efficiencies for the Far Forward Region for y dimension. 18

1 Introduction

PMCS_MUON is one of many packages within the PMCS framework. PMCS muon quickly simulates the properties of the muon detector geometry and gives each muon a gaussian smear in ϕ, η, and P_T. To acheive results that truely simulate the detector, we tune PMCS to the DØ monte carlo (MC) simulation.

2 Parameterization Methodology

To accuratly parameterize muons in PMCS, we must study the geometry of the muon detector. The DØ muon system can be broken down into three parts, a central region where $|\eta| \leq 1$, a forward region where $1 < |\eta| \leq 2$, and a far forward region where $|\eta| > 2$. Muons are parameterized differently depending on the region they are in.

Muons having $|\eta| \leq 1$ are parameterized with ϕ_{phys} and η_{phys}. Muons in the forward region are parameterized with ϕ_{phys}. While muons in the far forward region are parameterized with x and y.

The main method of tuning PMCS is to compare its results to the results of DØ*reco* over the same sample. We used $Z^{\circ}/\gamma \rightarrow \mu^+\mu^-$ events to determine the efficiency of DØ*reco* in both regions, and then tune PMCS_MUON to reproduce these efficiencies.

2.1 Matching Criteria

Both PMCS and DØ*reco* muons are compared to their generator counterparts. We calculate each muons' $\Delta\phi$ and $\Delta\eta$ from the MC generated muon. ΔR is defined as

$$\Delta R = \sqrt{\Delta\phi^2 + \Delta\eta^2} \tag{1}$$

A PMCS or DØ*reco* muon has a match if the ΔR angle it makes with its generated counterpart is less than 0.5. From this matching routine, we can determine the efficiency of a portion of the muon detector, and determine how to tune PMCS accordingly.

2.2 Detector Regions

Although there are generalized regions, specific parts of the detector were separated into subregions. These subregions are described in Table 1. The subregions were chosen because the detector efficiency in each subregion would be simple to model.

For the Central region, all ϕ outside of $4.32 \leq \phi \leq 5.10$ was modeled with a flat efficiency. For the detector between $4.32 \leq \phi \leq 5.10$, the feet (of the calorimeter) were modeled with flat efficiencies, except for subregion "Bottom Foot 2" which was modeled with a polynomial efficiency

For the Forward region, there are eight octants, each covering $\frac{\pi}{4}$ radians. Along the edges there are cracks in the detector. The segment bewteen $0.09 \leq (\phi \ mod \ \frac{\pi}{4}) \leq 0.70$ has a flat efficiency while the edges, $(\phi \ mod \ \frac{\pi}{4}) < 0.08$ and $(\phi \ mod \ \frac{\pi}{4}) > 0.71$ have linear efficiencies.

In the Far Forward Region, there is a square shaped hole near $|\eta| = 2$. Therefore the muons are parameterized with x and y. Muons with a $|x| < 95cm$ and $|y| < 95cm$ are modeled with a flat efficiency. Muons with $95cm \leq |x| \leq 115cm$ and $95cm \leq |y| \leq 115cm$ are modeled with a linear efficiency.

3 Comparison

We compare PMCS to DØ*reco* by running both on 19750 $Z^{\circ}/\gamma \rightarrow \mu^{+}\mu^{-}$ events. $Z^{\circ}/\gamma \rightarrow \mu^{+}\mu^{-}$ event were choosen because of their two isolated, high P_T muons. We used datasets generated with pythia p10.13.00, and run through DØ*gstar*, DØ*sim*, and DØ*reco* version p10.13.00. The name of the SAM dataset used is wz_zgamma_mumu_p1013_reco.

3.1 Matching Results

Again, all DØ*reco* muons and PMCS muons are matched to their closest generator counterpart. The $\Delta\phi$ graph is shown in Figure 1 and the $\Delta\eta$ graph is shown in Figure 2. Figure 3 shows the ΔR graph.

3.2 Tuning to DØ*reco*

First we compare the DØ*reco* muons to the generated muons to generate the efficiencies that we will tune PMCS to. The efficiency of different parts of the muon detector is determined by looking at the number of number of muons found in a subregion, and dividing by the total number of generator level muons in the same subregion.

For subregions modeled with a flat efficiency, the numbers generated from DØ*reco* are shown in Table 2.

For other subregions, we generated an efficiency plot and fitted the appropriate model to the curve. The results of these fits are shown in Figures 4 through 8. The results from the fits are shown in Table 3.

Figures 8 and 9 show the absolute value of x and y respectivly for the subregion around the edge of the hole in the muon detector.

3.3 Efficiency Plots

Now with efficiencies modeled for all the regions, we can compare how PMCS performs against DØ*reco*. Figures 9 through 13 show efficiency plots for all the regions in Table 1. Some of the subregions are combined into a single graph. Figure 9 shows the general central subregion and the efficiencies of PMCS and DØ*reco*. Figure 10 shows all the bottom hole subregions, from $0 \leq |\eta| \leq 1.0$.

For the Forward region, Figure 11 shows the efficiency for all eight segments ($\phi \, mod \, \frac{\pi}{4}$), from 0 to $\frac{\pi}{4}$. It shows how both edges and the flat region algorithms compare.

In the Far Forward region, Figure 12 shows the x efficiency and Figure 13 shows the y efficiency. For each dimention, the abolute value of x (or y) is graphed. Both ends of the muon detector are used for the plot. The units of x and y are in cm.

4 Resolutions

After PMCS_MUON determines muon acceptances, it smears each muon's ϕ, η, and $\mathrm{P_T}$. The ϕ and η resolutions are simple gaussians:

$$\phi_{smear} = \phi \ \times x \tag{2}$$

$$\eta_{smear} = \eta \ \times x \tag{3}$$

Where x is a random gaussian number between -1 and 1. The $\mathrm{P_T}$ resolution is more complex. The energy resolution smears the muons with $\frac{1}{p}$ with the following formula.

$$If|\eta| < 1 \ \ \mathrm{P_T}_{smear} = \frac{\mathrm{P_T}}{(1 - x \times (0.0044\mathrm{P_T} \oplus 0.2506))} \tag{4}$$

$$If|\eta| \geq 1 \ \ \mathrm{P_T}_{smear} = \frac{\mathrm{P_T}}{(1 - x \times (0.001905\mathrm{P_T} \oplus 0.255))} \tag{5}$$

Again, x is a random gaussian number. Since PMCS also uses a particle's track information to determine the muon's ϕ, η, and $\mathrm{P_T}$, and this tracking data are better, they are used to fill the output chunk. In effect, PMCS_MUON's algorithm is only used to determine muon acceptance.

5 Conclusion

Since the tracking chamber resolves the muon's ϕ, η, and $\mathrm{P_T}$ much better than the muon detector, PMCS_MUON's main goal is to accuractely model the efficiency of the detector. This current PMCS_MUON algorithm has many improvements since the last tune. Different regions of the detector are modeled differently. Each of the detector subregions has its own muon efficiency. This results a better muon detection routine.

6 Acknowledgements

We would like to thank, in no particular order:
Marco Verzocchi
Daria Zieminska
Gavin Hesketh
Ton Diehl
Andrzej Zieminski

Central Region			
Description	η constraint	ϕ constraint (rad)	Model
General Central Subregion	$0 \leq \lvert\eta\rvert \leq 1$	$\phi < 4.32$ OR $\phi > 5.10$	flat
Bottom Central	$0 \leq \lvert\eta\rvert \leq 0.35$	$4.32 \leq \phi \leq 5.10$	flat
Bottom Foot 1	$0.35 < \lvert\eta\rvert \leq 0.55$	$4.32 \leq \phi \leq 5.10$	flat
Between Feet	$0.55 < \lvert\eta\rvert \leq 0.65$	$4.32 \leq \phi \leq 5.10$	flat
Bottom Foot 2	$0.65 < \lvert\eta\rvert \leq 0.95$	$4.32 \leq \phi \leq 5.10$	parabolic
Bottom Edge	$0.95 < \lvert\eta\rvert \leq 1.00$	$4.32 \leq \phi \leq 5.10$	flat
Forward Region			
Description	η constraint	ϕ constraint (rad)	Model
Segment Edge 1	$1 < \lvert\eta\rvert \leq 2$	$(\phi \; mod \; \frac{\pi}{4}) < 0.08$	linear
Middle of Segment	$1 < \lvert\eta\rvert \leq 2$	$0.08 \leq (\phi \; mod \; \frac{\pi}{4}) \leq 0.71$	flat
Segment Edge 2	$1 < \lvert\eta\rvert \leq 2$	$(\phi \; mod \; \frac{\pi}{4}) > 0.71$	linear
Far Forward Region			
Description	x constraint (cm)	y constraint (cm)	Model
Middle of Hole	$\lvert x\rvert < 95$	$\lvert y\rvert < 95$	flat
Edge of Hole	$95 \leq \lvert x\rvert \leq 115$	$95 \leq \lvert y\rvert \leq 115$	linear

Table 1: Breakdown of Detector Regions for PMCS. Note that flat is not the same as linear.

Subregion	*Efficiency*
Central Region	
General Central	0.972 ± 0.00131
Bottom Central	0.763 ± 0.0145
Bottom Foot 1	0.526 ± 0.0228
Between Feet	0.843 ± 0.0248
Bottom Edge	0.777 ± 0.0152
Forward Region	
Middle of Segment	0.978 ± 0.00141
Far Forward Region	
Middle of Hole	0.0832 ± 0.00318

Table 2: Efficiencies for Subregions modeled with flat efficiency.

Subregion	$p0$	$p1$	$p2$
Central Region			
Bottom Foot 2	20.501	−51.163	32.342
Forward Region			
Segment Edge 1	0.0468	17.400	
Segment Edge 2	14.698	−18.713	
Far Forward Region			
Edge of Hole	−5.638	0.0593	

Table 3: Results of Fits to Subregions of muon detector.

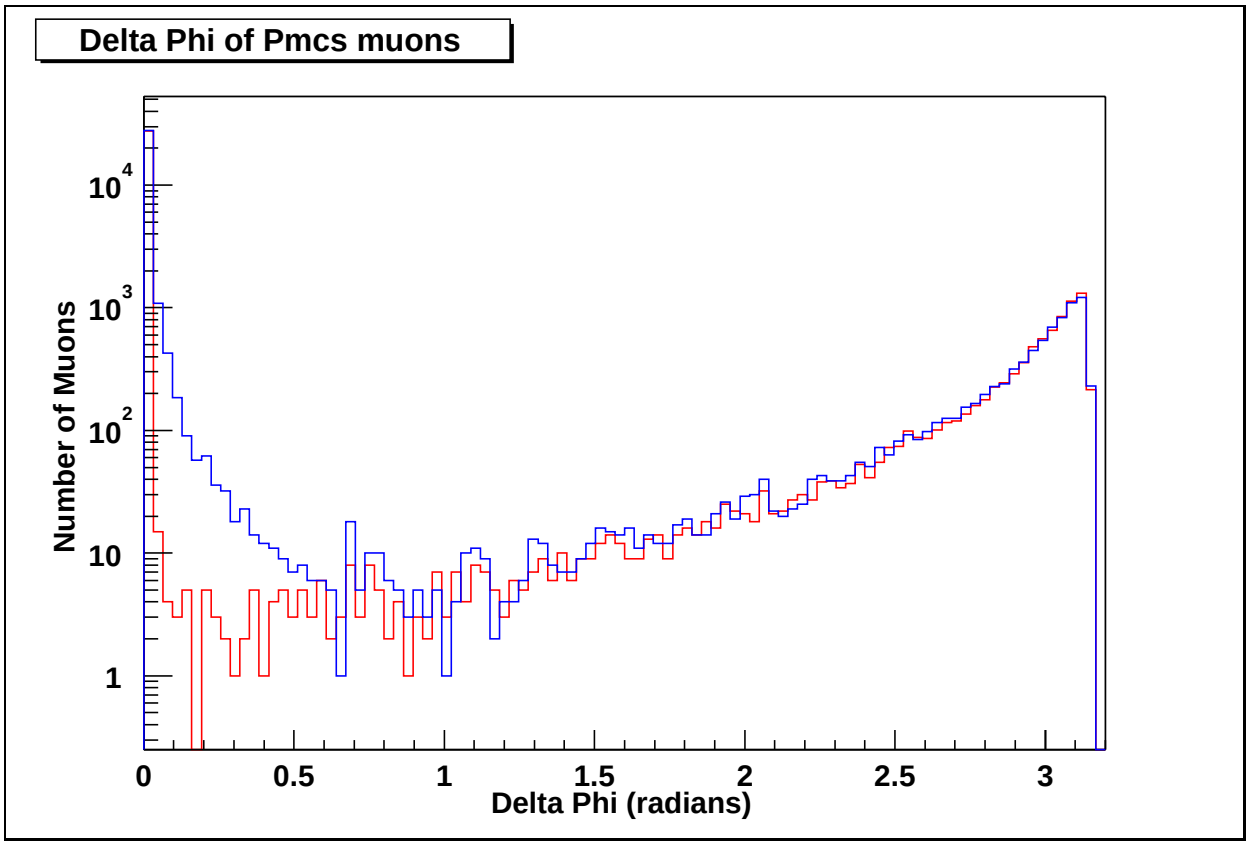

Figure 1: $\Delta\phi$ comparing PMCS to MC muons and DØ*reco* to MC muons. PMCS muons are drawn with red. DØ*reco* muons are drawn with blue.

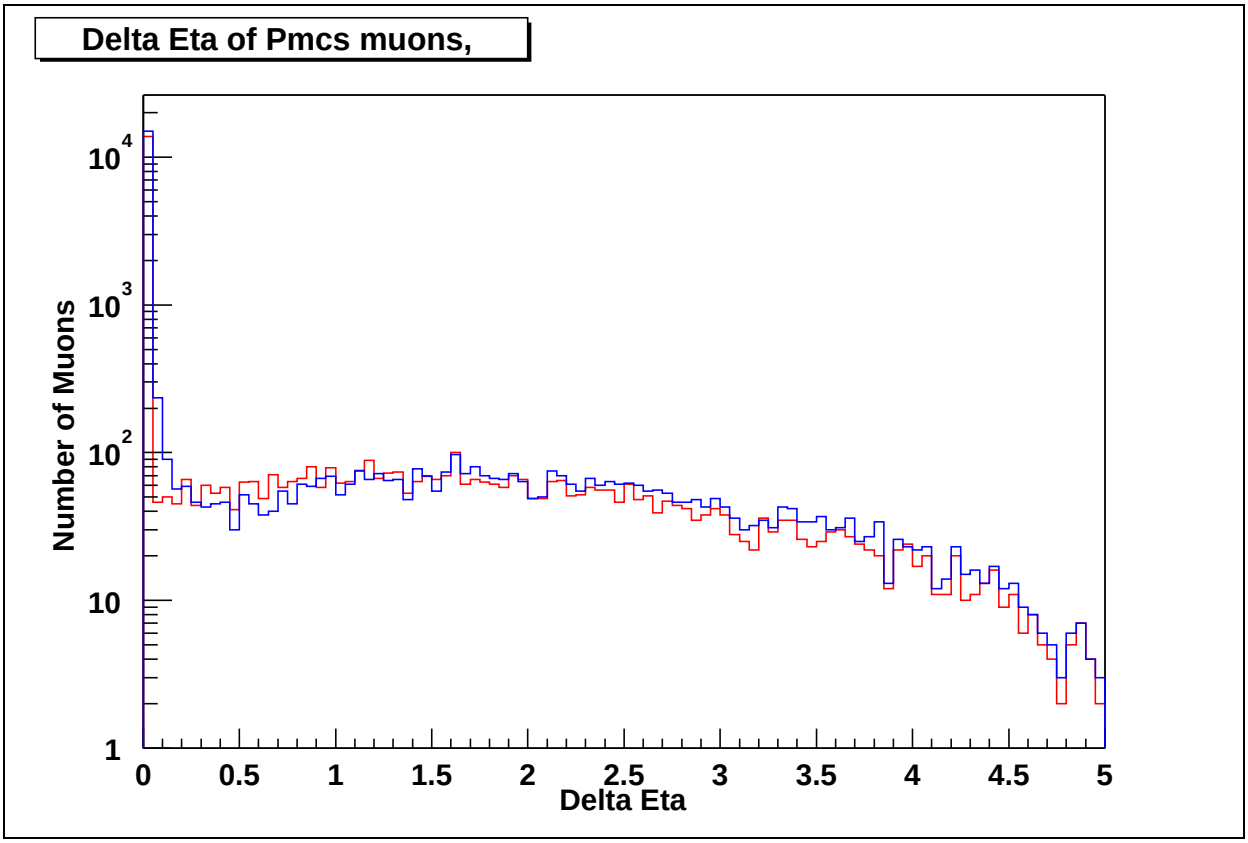

Figure 2: $\Delta\eta$ comparing PMCS to MC muons and DØ*reco* to MC muons. PMCS muons are drawn with red. DØ*reco* muons are drawn with blue.

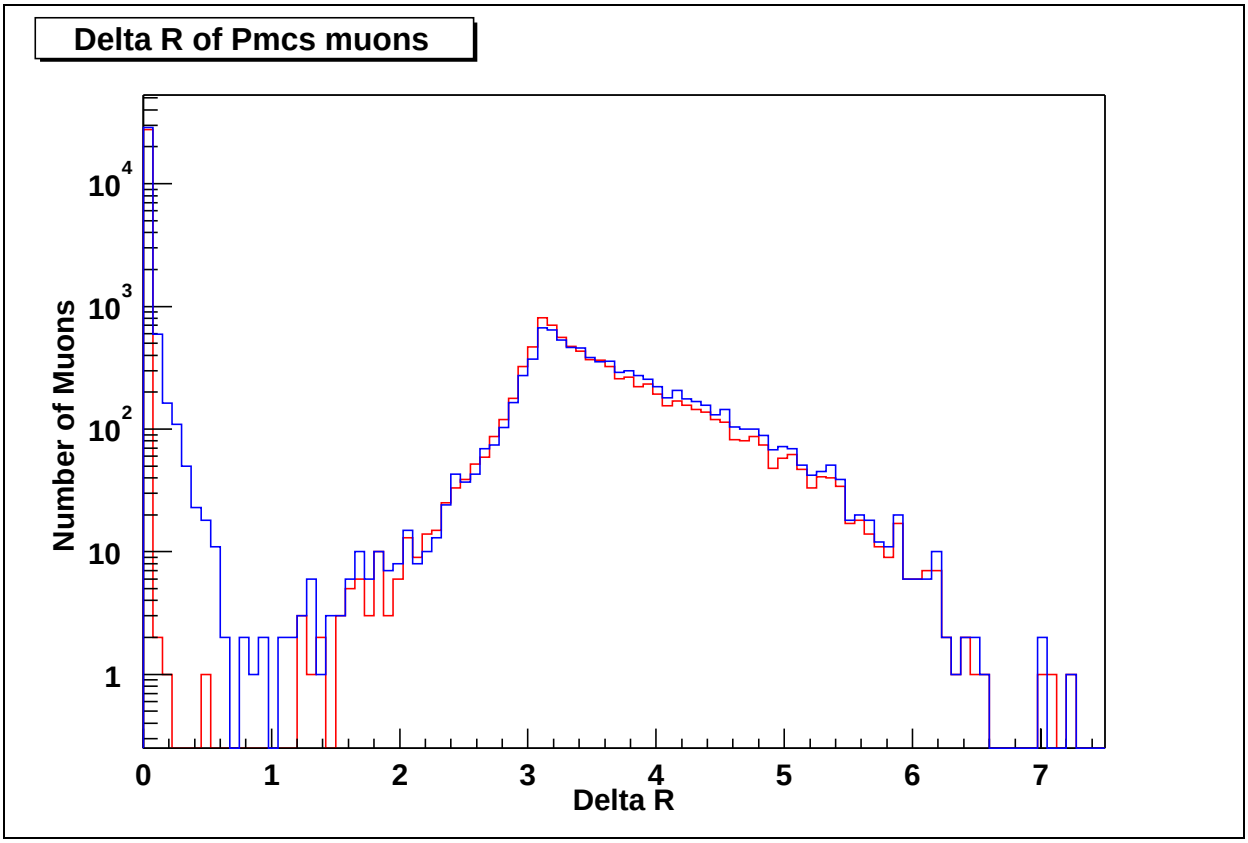

Figure 3: ΔR comparing PMCS to MC muons and DØ*reco* to MC muons. PMCS muons are drawn with red. DØ*reco* muons are drawn with blue.

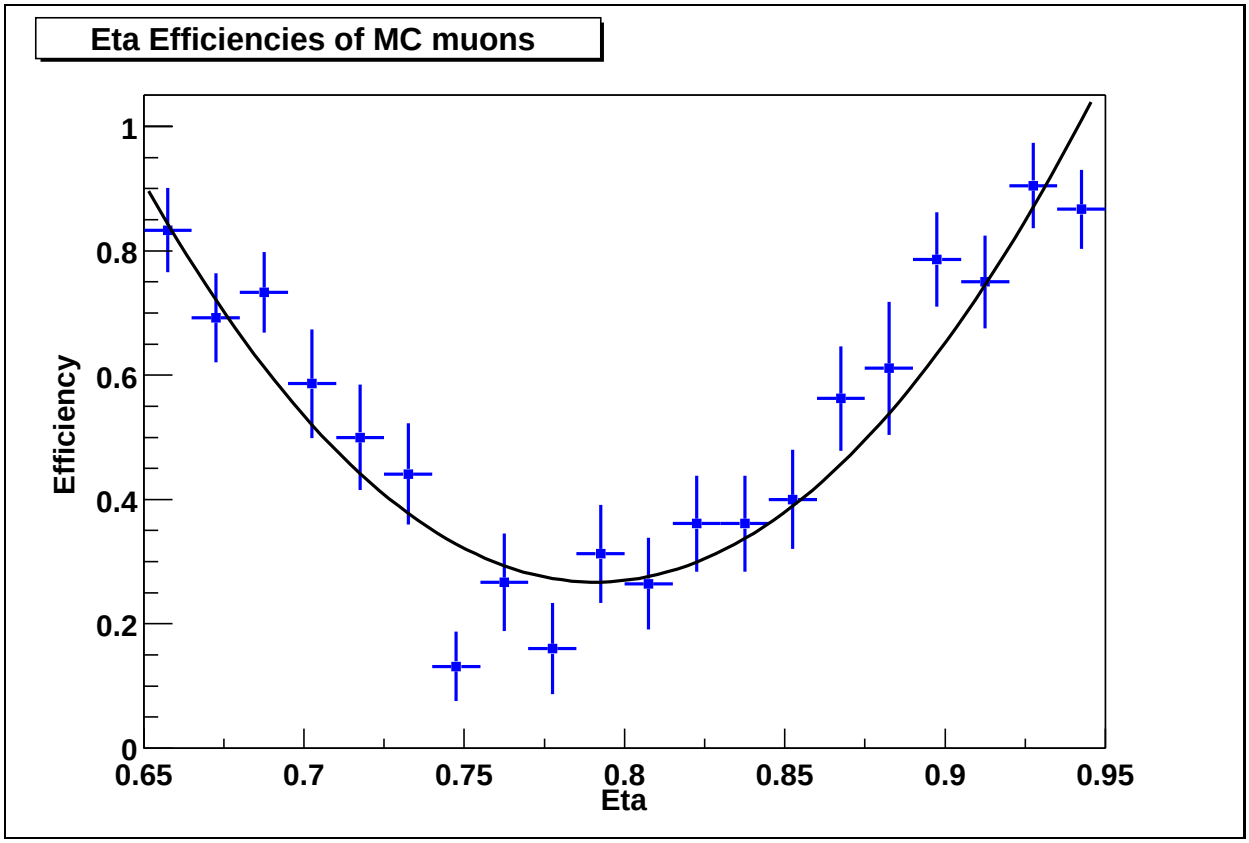

Figure 4: Fit of Efficieny of Subregion Bottom Foot 2: $0.65 < |\eta| \leq 0.95$ and $4.32 \leq \phi \leq 5.10$.

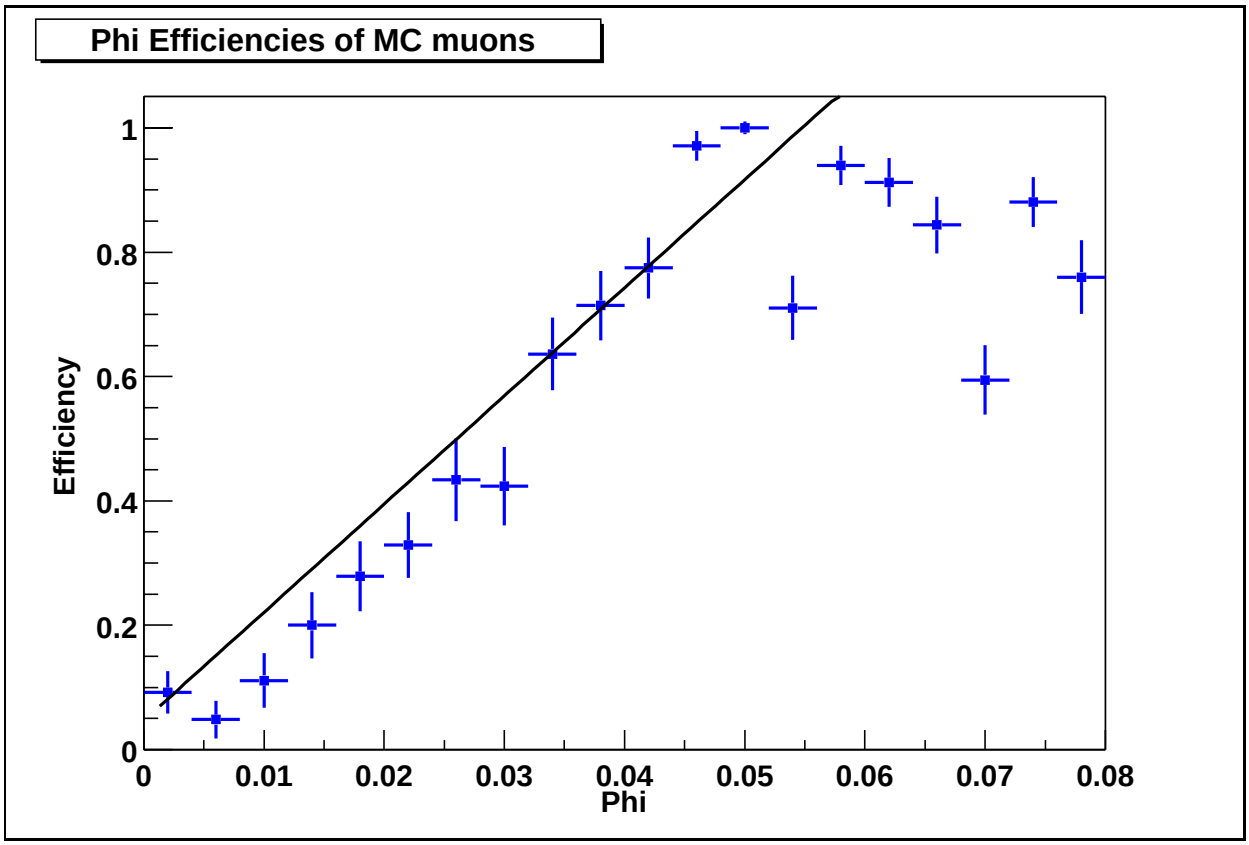

Figure 5: Fit of Efficiency of Subregion edge of segment: $1.0 < |\eta| \leq 2.0$ and $\phi \; mod \; \frac{\pi}{4} < 0.08$.

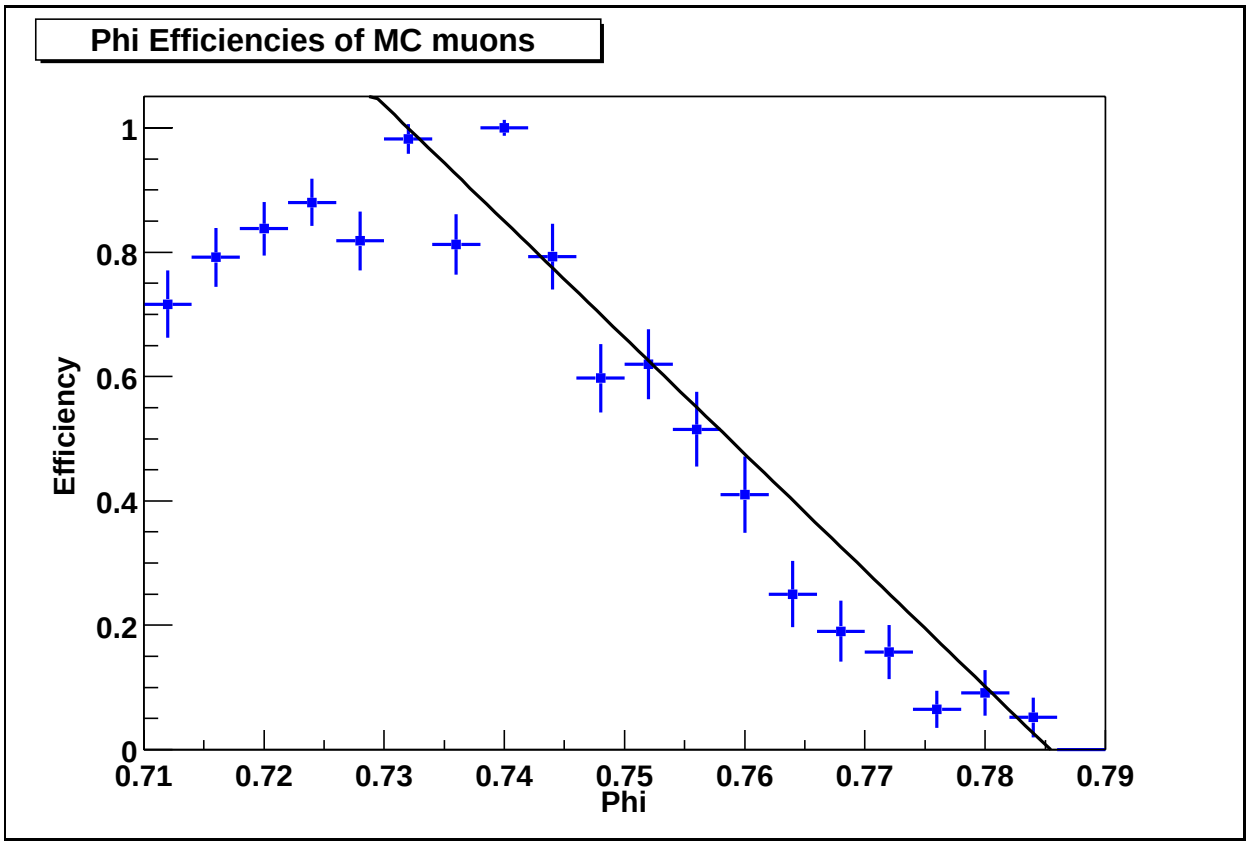

Figure 6: Fit of Efficiency of Subregion edge of segment :$1.0 < |\eta| \leq 2.0$ and $\phi \; mod \; \frac{\pi}{4} > 0.71$.

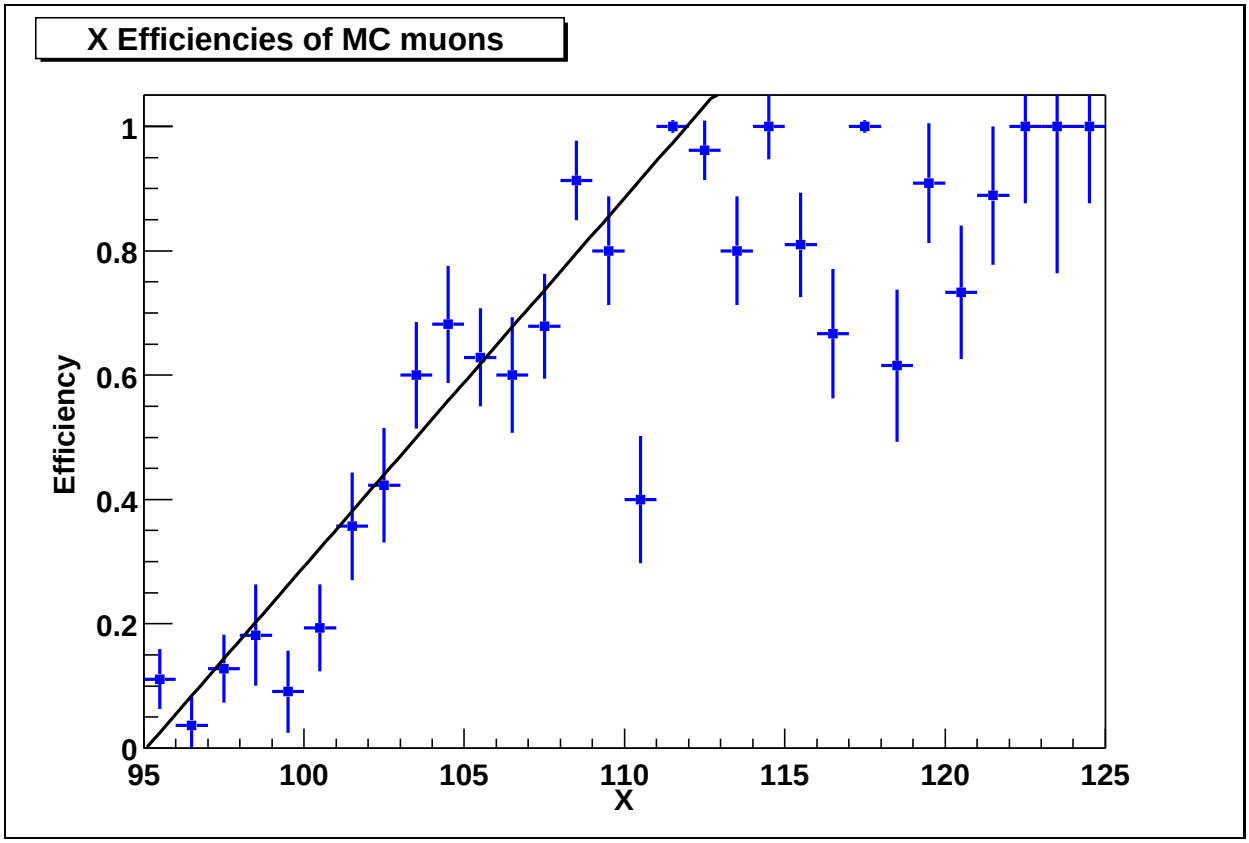

Figure 7: Fit of Efficiency Subregion of edge of hole : $|\eta| > 2.0$ and $95 \leq |x| \leq 115$.

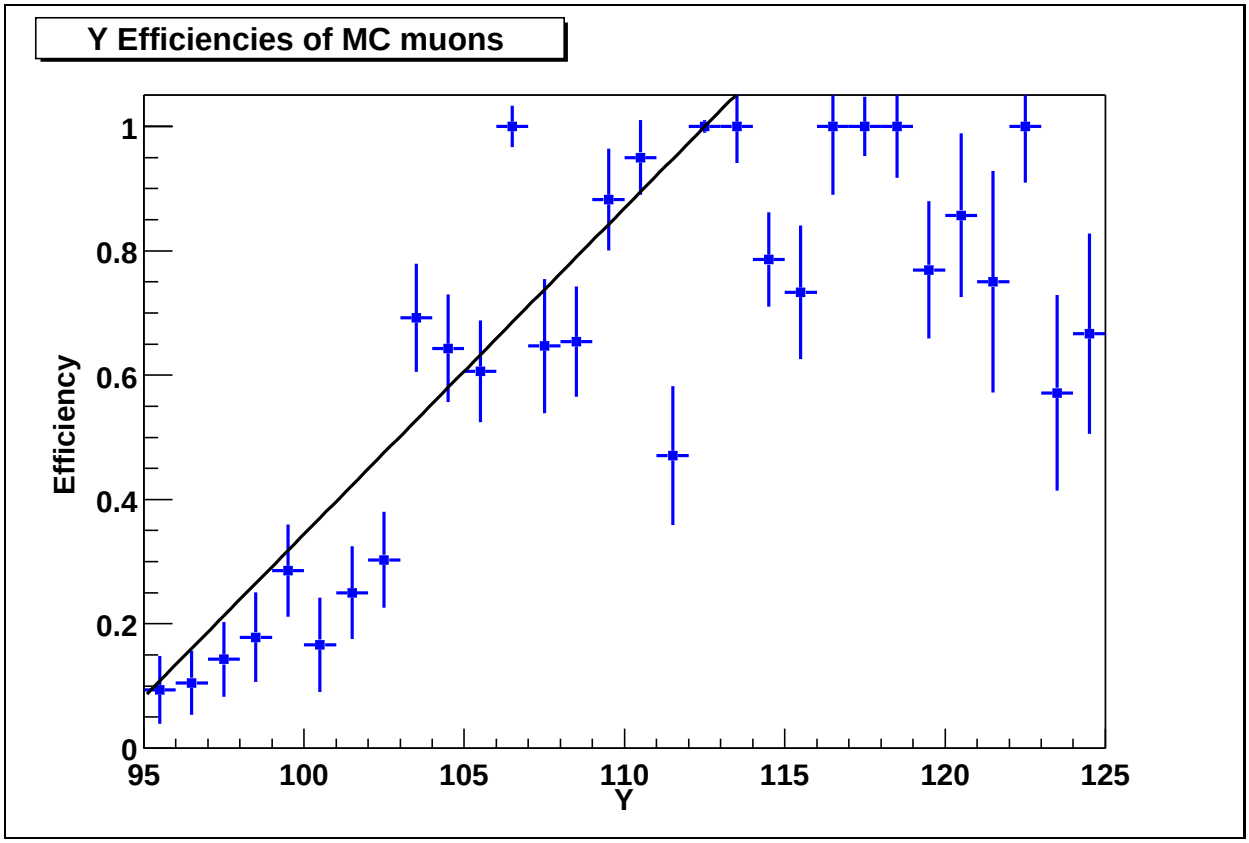

Figure 8: Fit of Efficiency of edge of hole subregion: $|\eta| > 2.0$ and $95 \leq |y| \leq 115$.

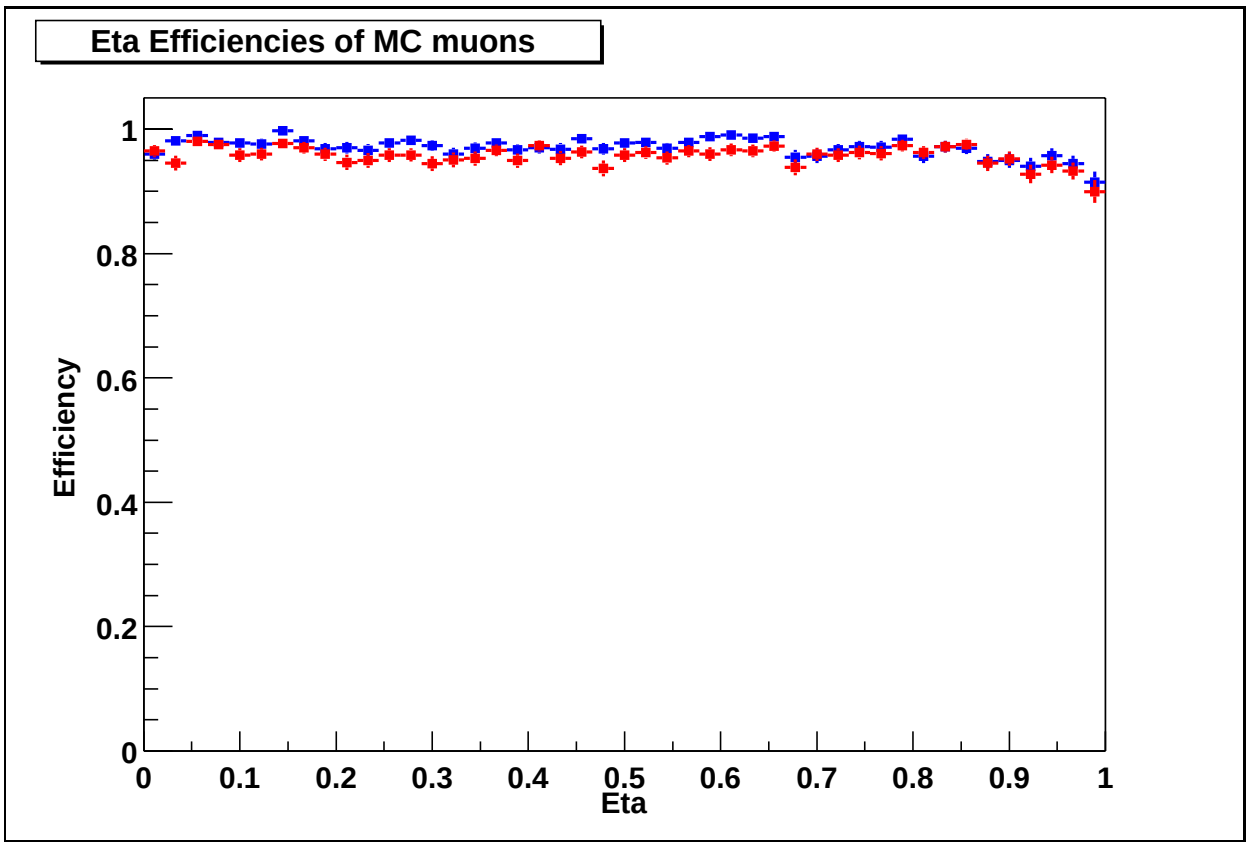

Figure 9: Comparison between PMCS and DØ*reco* muons in the Central Region, general central subregion. PMCS muons are drawn with red. DØ*reco* muons are drawn with blue.

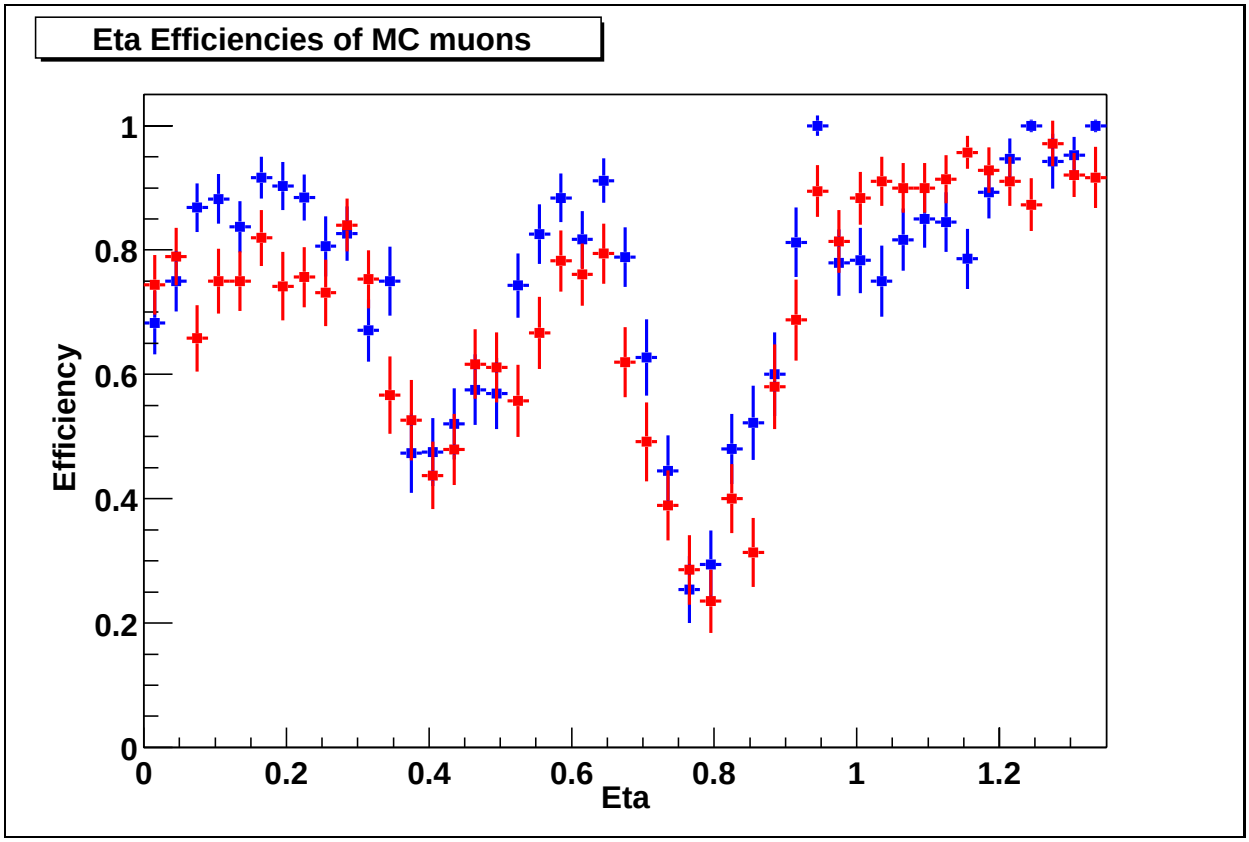

Figure 10: Efficiency of Central Region, $4.32 \leq \phi \leq 5.10$ *only*, representing the bottom hole subregions. PMCS muons are drawn with red. DØ*reco* muons are drawn with blue.

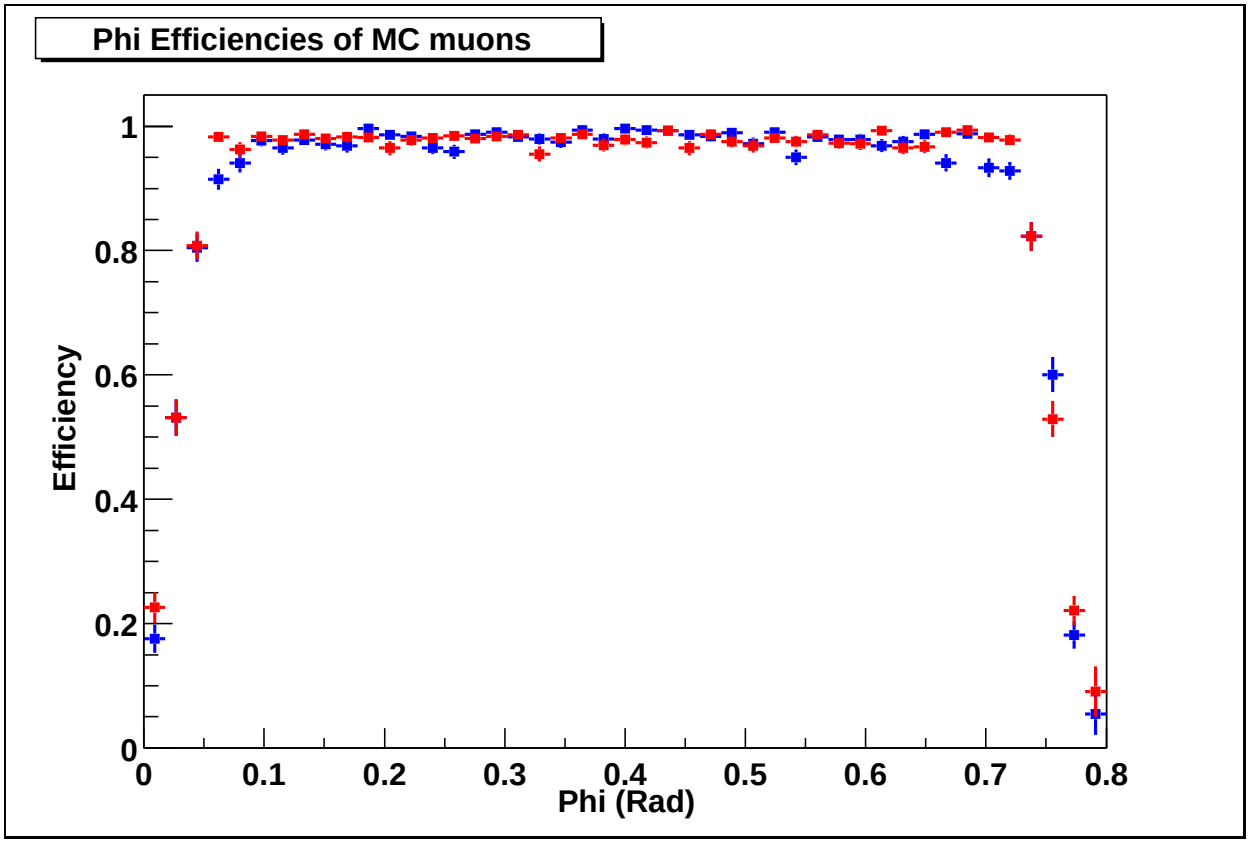

Figure 11: Efficiency of the Forward Region, ϕ *mod* $\frac{\pi}{4}$, representing all eight segments. PMCS muons are drawn with red. DØ*reco* muons are drawn with blue.

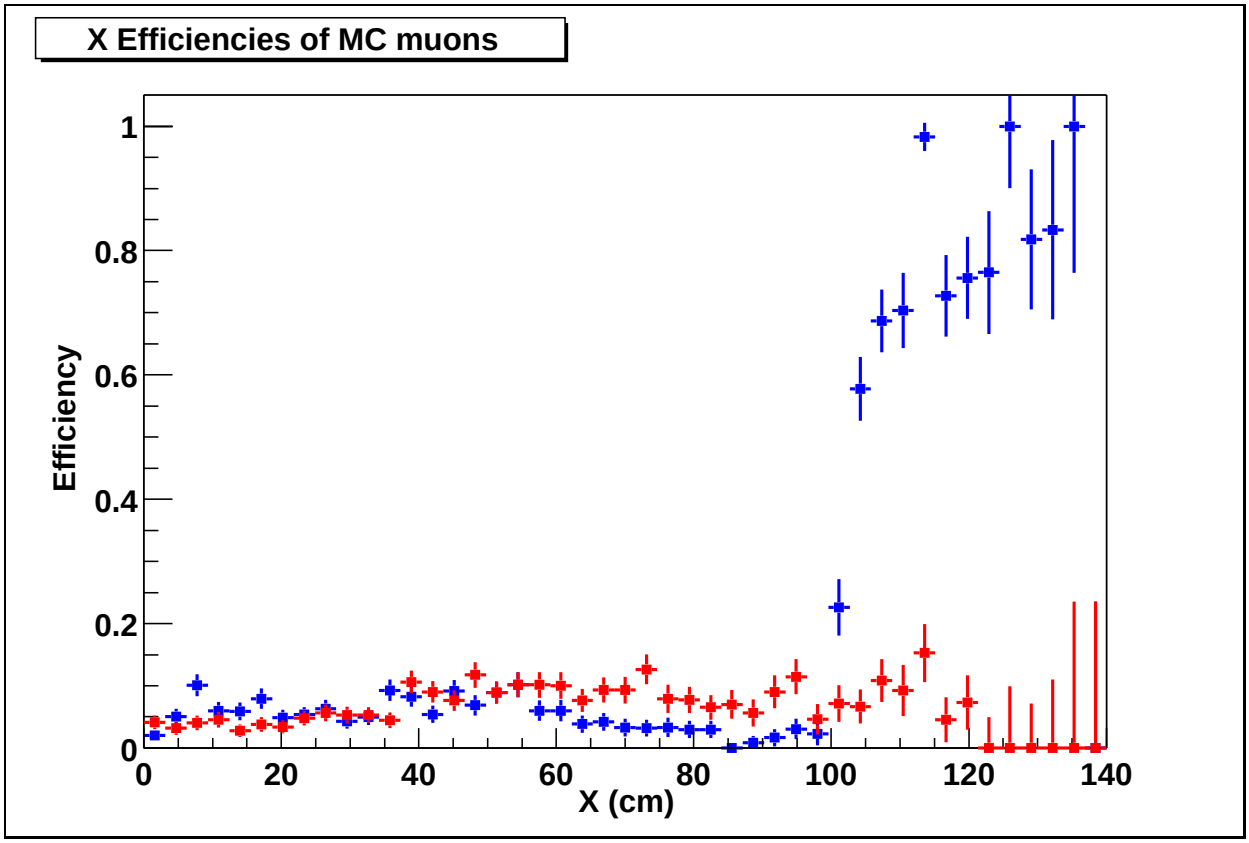

Figure 12: Efficiency of the Far Forward Region for x dimension. PMCS muons are drawn with red. DØ*reco* muons are drawn with blue.

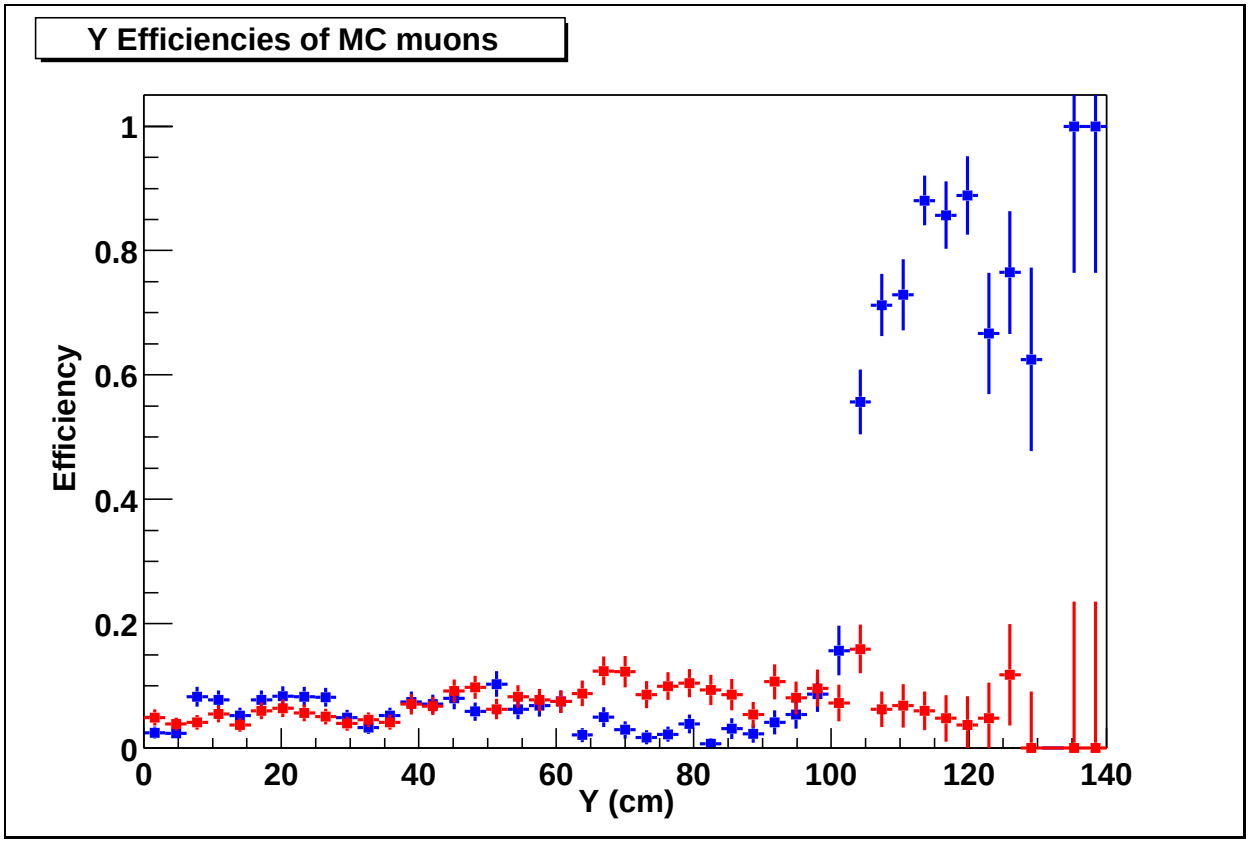

Figure 13: Efficiency of the Far Forward Region for y direction. PMCS muons are drawn with red. DØ*reco* muons are drawn with blue.